Available online at www.sciencedirect.com
SCIENCE DIRECT
Journal of Molecular Catalysis A: Chemical 238 (2005) 26–34
JOURNAL OF MOLECULAR CATALYSIS A: CHEMICAL
www.elsevier.com/locate/molcata

Generation of size-controlled palladium(0) and gold(0) nanoclusters inside the nanoporous domains of gel-type functional resins Part II: Prospects for oxidation catalysis in the liquid phase

C. Burato [a], P. Centomo [a], G. Pace [b], M. Favaro [c], L. Prati [d,*], B. Corain [a,b,*]

[a] *Dipartimento di Scienze Chimiche, via Marzolo 1, 35131 Padova, Italy*
[b] *Istituto di Scienze e Tecnologie Molecolari, C.N.R., Sezione di Padova c/o, Dipartimento di Scienze Chimiche, Via Marzolo 1, 35131 Padova, Italy*
[c] *Istituto di Chimica Inorganica e delle Superfici, C.N.R., Corso Stati Uniti 4, 35131 Padova, Italy*
[d] *Dipartimento di Chimica Inorganica Metallorganica Analitica, Università degli Studi di Milano, Via Venezian, 21, 20133 Milano, Italy*

Received 28 December 2004; received in revised form 20 April 2005; accepted 20 April 2005
Available online 14 June 2005

Abstract

Moderately cross-linked co-polymers of *N*,*N*-dimethylacrylamide (DMAA), 2-(methylthio)ethyl methacrylate (MTEMA)and *N*,*N*′-methylenebisacrylamide proves to be effective macromolecular ligands able to extract, Pd^{II} and Au^{III} from water solutions and to thoroughly disperse them inside the relevant polymer frameworks. Chemical reduction with $NaBH_4$ in water leads to M^0/resin composites, in which size-control of the generated metal nanoclusters is achieved. Catalysts Au^0/MTEMA-DMAA are active in the rapid oxidation of *n*-butanal to *n*-butanoic acid by dioxygen under mild conditions in water. Catalysts M^0/MTEMA-DMAA and M^0/C (M = Au, Pd) are active and moderalely chemoselective in the oxidation of *n*-butanol to *n*-butanal under the same conditions. Activity and chemoselectivity are positively affected by the co-presence of the two metal centres and for M^0 = Au and reach the best level when the very hydrophilic resin poly-(4-vinylpyridine-acrylic acid-*N*,*N*′-methylenebisacrylamide) (VAM) is employed.

Keywords: Pd^0; Au^0 nanoclusters; Functional resins; Oxidation catalysis

We have recently reported in this Journal on the synthesis of Au^0/resins and Pd^0/resins nanocomposites, M^0/S; M = Pd, Au; S = functional resin), in which size-controlled metal nanoclusters (ca. 2.5 nm) are produced inside- nanostructurally well-characterized gel-type polyacrylic resins, i. e. poly-2-(methylthio)ethyl methacrylate–*N*,*N*-dimethylacrylamide–*N*,*N*′-methylenebisacrylamide (4–88–8 mol%) hereafter referred to as MTEMA-DMAA-4–8 [1]. In Ref. [1], we provide an adequate presentation of the reasons that qualify these innovative supported metal catalysts as well as a large selection of our related literature. Moreover, we have also presented both arguments about and supporting evidence for the physical role played by the polymer framework in exerting a geometrical control on the size of the produced M^0 nanoclusters [2a,b], as shown in Fig. 1.

We herein report on the synthesis of other Au^0/S, and Pd^0/S nanocomposites based on resins that are closely related to MTEMA-DMAA-4–8 and on a series of catalytic tests concerning the oxidation of *n*-butanal to carboxylic acids and of *n*-butanol to *n*-butanal with dioxygen in water under very moderate temperature and pressure conditions.

1. Experimental

1.1. Apparatus

XRM. Cambridge Stereoscan 250 EDX PW 9800. *TEM*. PHILIPS CM 200 FEG with a Supertwin-Lens operated

* Corresponding authors. Tel.: +39 049 8275211; fax: +39 049 8275223.
E-mail address: benedetto.corain@unipd.it (B. Corain).

1381-1169/$ – see front matter © 2005 Elsevier B.V. All rights reserved.
doi:10.1016/j.molcata.2005.04.062

Table 1
Details on the synthesis and on experimental elemental composition of resins MTEMA-DMAA-4–4, MTEMA-DMAA-4–6, MTEMA-DMAA-4–8, MTEMA-DMAA-10–4, VAM

Code	Monomers (g)	C (%)	H (%)	N (%)	S (%)
MTEMA-DMAA-4–4	MTEMA (0.86), DMAA (11.86), MBAA (0.84)	56.6	8.9	12.7	1.5 (0.46)[a]
MTEMA-DMAA-4–6	MTEMA (0.82), DMAA (11.42), MBAA (1.19)	57.2	9.9	12.9	1.2 (0.38)[a]
MTEMA-DMAA-4–8	MTEMA (0.81), DMAA (11.12), MBAA (1.57)	56.6	8.9	13.2	1.4 (0.44)[a]
MTEMA-DMAA-10–4	MTEMA, DMAA, MBAA	54.7	11.1	8.8	3.4 (1.06)[a]
VAM	MA (12.2), VP (1.7), MBAA (1.95)	53.8	7.4	1.7	–

DMAA: *N*,*N*-dimethylacrylamide; MTEMA: 2-(methylthio)ethyl methacrylate; MBAA: *N*,*N*′-methylenebisacrylamide; VP: 4-vinylpyridine; MA: methacrylic acid
[a] mmol/g of MTEMA.

at an accelerating voltage of 200 KeV. Lens parameters: $f = 1.7$ mm, $C_s = 1.2$ mm, $C_c = 1.2$ mm, giving a point resolution of 0.24 nm and a line resolution of 0.1 nm. *ISEC*. Home-assembled apparatus made available by Dr. K. Jerabek, Institute of Chemical Process Foundamentals, Czech Academy of Sciences (Prague-Suchdol). Basic operations and choice of steric probes are described in Ref. [3].

Samples preparation for TEM. Some samples were obtained by mechanical milling of the as-prepared solid sample and subsequent dispersing in ethanol with an ultrasonic bath for 0.5 h. One drop of thus obtained suspension was brought onto a carbon-coated copper grid, dried at room temperature and then put into the microscope. Some samples were obtained by embedding the material in Araldite CY212 and, after polymerization, by cutting 70 nm slices with a diamond-knife.

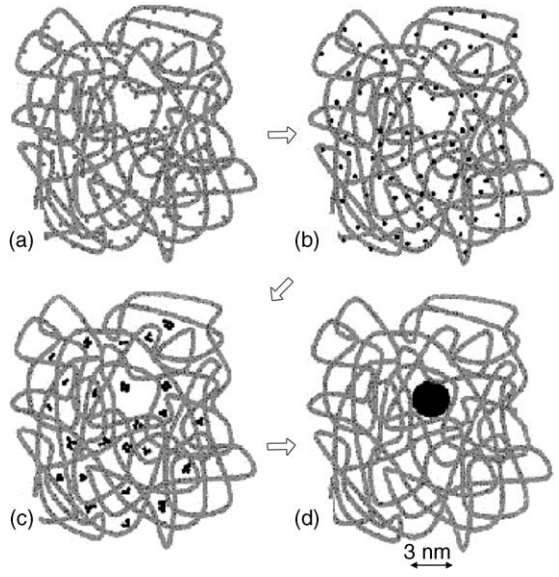

Fig. 1. Generation of size-controlled metal nanoparticles inside metallated resins: our template controlled synthesis approach (TCS). Macromolecular chains are interconnected by cross-linking short chains (not shown in the sketch). The Figure depicts a two-dimension section of a spheroidal volume element ca. 20 nm in diameter. (a) Pd^{II} is homogeneously dispersed inside of the polymer framework; (b) Pd^{II} is reduced to Pd^0; (c) Pd^0 atoms start to aggregate in subnanoclusters; (d) a single 3 nm nanocluster is formed and "blocked" inside the largest mesh present in that "slice" of polymer framework [2a] (From Ref. [2a], with permission).

Solvents and chemicals. From various commercial sources, used as received.

Syntheses. The synthetic procedure for functional resins is described in various previous papers from these Laboratories. The reader is particularly referred to Ref. [4]. The only innovation that was recently introduced is the washing procedure of the ground and sieved materials, i.e. a thorough treatment with methanol in a Soxhlet apparatus for 4 days, followed by conventional drying at 5 Torr, 60 °C for 24 h. Specific synthesis details are collected in Table 1.

Elemental analyses listed in Table 2 are very close to the expected composition (next section), for a 100% yield, after accounting for absorbed water (from 5.0 to 5.5%).

1.2. Metallation of functional resins and reduction to resin/M^0 composites

Metallation of functional resins and reduction to resin/M^0 composites (typical procedure). ca. 1 g of functional resin (ca. 0.4 mmol –SMe; ca. 1.0 mmol VP) is suspended in 40 ml of

Table 2
Designed composition and observed polymerisation yields of resins MTEMA-DMAA-4-4, MTEMA-DMAA-4–6, MTEMA-DMAA-4–8, MTEMA-DMAA-10–4 and VAM

Code	Monomer composition	mol%	Polymerisation yield (%)
MTEMA-DMAA-4–4	DMAA	92	99
	MTEMA	4	
	MBAA	4	
MTEMA-DMAA-4–6	DMAA	90	98
	MTEMA	4	
	MBAA	6	
MTEMA-DMAA-4–8	DMAA	88	99
	MTEMA	4	
	MBAA	8	
MTEMA-DMAA-10–4	DMAA	86	97
	MTEMA	10	
	MBAA	4	
VAM	MA	92	95
	VP	4	
	MBAA	4	

DMAA: *N*,*N*-dimethylacrylamide; MTEMA: 2-(methylthio)ethyl methacrylate; MBAA: *N*,*N*′-methylenebisacrylamide; VP: 4-vinylpyridine; MA: methacrylic acid.

the required medium (see below) and left under moderate stirring for 2 h. ca. 20 mg (0.06 mmol) of $AuCl_3$ in 40 ml MeCN or ca. 25 mg (0.11 mmol) of $Pd(OAc)_2$, in 2:1 THF/water or 1.6 mg of $PdCl_2$ (0.09 mmoli) and 0.05 g of NaCl in 40 ml water are added under manual stirring and left under moderate mechanical stirring for ca. 4 days, after which time the surnatant phase turns out to be colourless. The resin colour does not appreciably change in the case of Au and turns to pale brown in the case of Pd. Metallated and reduced resins are recovered upon filtration, washed with water and dried in vacuo at 60 °C to constant weight.

1.3. Reduction of metallated resins in water

Reduction of metallated resins in water (typical procedure). The metallated resin (ca. 1 g) is suspended in ca. 200 ml water and left under moderate stirring for 2 h. 250 mg (6.6 mmol) of $NaBH_4$ dissolved in 50 ml water are added under manual stirring with consequent vigorous gas evolution, and left under moderate mechanical stirring for ca. 90 min, after which time the surnatant phase appears to be colourless and the resins have become burgundy red (Au) and black (Pd). Reduced resins are filtered, washed with water and dried in vacuo at 60 °C to constant weight.

1.4. Catalytic tests

Oxidation of *n*-butanal and of *n*-butanol are carried out at 70 °C in a 30 ml glass reactor equipped with heater, mechanical stirrer, gas supply and thermometer. The reactor is charged with the water solution of the substrate (0.3 M, base/alcohol molar ratio equal to 1 for *n*-butanol oxidation). The reactor is pressurizes at 3 atm with dioxygen at room temperature. When the temperature reaches 70 °C, the reactor is connected to a source of gas that provides a constant oxygen pressure equal to 3 atm. Samples are periodically withdrawn and are analyzed with HPLC (column Alltech OA-10308, 300 mm × 7.8 mm, UV and refractive index detectors) by employing H_3PO_4 0.1% as eluting medium. Blank experiments show that *n*-butanal is reasonably stable (less than 6% decomposition) in the employed alkaline solutions for at least 2 h.

2. Results and discussion

We designed three functional supports hereafter referred to as MTEMA-DMAA-4–4, MTEMA-DMAA-4–6, MTEMA-DMAA-4–8 (see Table 2 for relevant coding) aimed at dispersing Au^0 and Pd^0 nanoclusters, expected to be featured by different and controlled size. The choice of three different cross-linking degrees rests on the expectation of a consequent influence on the overall porosity of the polymer framework. Resin MTEMA-DMAA-10–4 was synthesized for hosting simultaneously Au^0 and Pd^0 nanoclusters. Resin VAM was synthesized and employed for supporting Au^0 in view of its very large water compatibility (7.4 ml/g in sodium form).

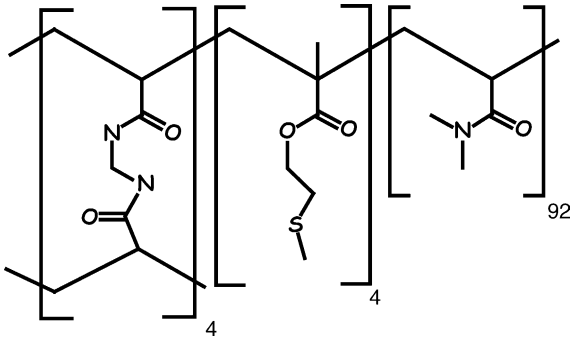

Fig. 2. Primary structure of resin MTEMA-DMAA-4–4.

Resins design and composition and relevant polymerisation yields are reported in Table 2.

Quite in line with our longstanding experience [5e,h], co-polymerization of the employed monomers and cross-linker promoted by γ-rays leads to the facile and quantitative conversion to the desired materials bearing ca. 0.4 mmol/g of thiomethyl functionality (ca. 0.28 mmol/g for MTEMA-DMAA-10–4) (Fig. 2). Resins are obtained as 180–400 μm brittle colourless and transparent particles (see Section 1) with a reasonable swellability in water and methanol (2–3 ml/g) and a lower swellability in acetonitrile (ca. 0.7 ml/g).

The choice of monomer 2-(methylthio)ethyl methacrylate (MTEMA) was suggested by the reasonable expectation that the thioethereal functionality be a useful ligating site for anchoring of both Au^{III} and Pd^{II} to the functional resin and as a means of homogeneous dispersion of the metal centers (and consequently of Au^0 and Pd^0 nanoclusters, Fig. 1) through the body of the resin particles in the synthetic steps 1–2. The thioethereal functions are also feasible as stabilizing sites for the Au^0 nanoclusters thus preventing sintering trends.

In fact, all resins react readily with $AuCl_3$ in MeCN, with $Pd(OAc)_2$ in THF/H_2O 2:1 and with $[PdCl_4]^{2-}$ in water to give brown colourless and light brown materials, respectively, which are subsequently reduced with $NaBH_4$ in water to give red (Au) and black (Pd) materials, respectively (Table 3):

$$Ⓟ\text{-S(Me)} + Au^{III}\,(aq) \rightarrow Ⓟ\text{-S(Me)-}Au^{III,I}\,(s) \quad (1)$$

$$Ⓟ\text{-S(Me)-}Au^{III,I}\,(s) + BH_4^- \rightarrow Ⓟ\text{-S(Me)/}Au^0\,(s) + \text{products} \quad (2)$$

Resins MTEMA-DMAA-4–4, MTEMA-DMAA-4–6, MTEMA-DMAA-4–8 were analysed with inverse steric

Table 3
Analytical data for Au^0/resin, Pd^0/resin and Au^0/Pd^0/resin composites

Code	Au (%)	Pd (%)	Colour
MTEMA-DMAA-4–4/M	0.85	0.73	Burgundy red (Au), black (Pd)
MTEMA-DMAA-4–6/M	0.67	0.85	Burgundy red (Au), black (Pd)
MTEMA-DMAA-4–8/M	0.75	0.70	Burgundy red (Au), black (Pd)
MTEMA-DMAA-10–8/M	1.61	2.43	Black (Au + Pd)
VAM/M	0.15	–	Red

exclusion chromatography (ISEC) and relevant M^0/resin composites were characterised with XRMA and with TEM.

2.1. ISEC analysis

ISEC [5f,6,8] provides careful information on the nanometer scale morphology of a given resin, after its swelling in a convenient liquid medium. It is based on measurements of elution behaviour of standard solutes with known effective molecular size that are let to flow through a column filled with the investigated material at conditions in which the elution is influenced exclusively by the (nano)morphology of the stationary phase. Similarly to the case of the other porosimetric methods, mathematical treatment of the elution data allows one to obtain information on the morphology of the investigated material using a simple geometrical model. It is now established that for describing the morphology of swollen polymer gels the best suitable tool is the so-called Ogston's model [7] that depicts pores as spaces between randomly oriented solid rods. This geometry, albeit a fair simplification of the morphology of swollen polymer networks, provides a faithful description of both the intensive parameters (polymer chain densities) and extensive properties (specific volumes of variously dense polymer fractions). On the other hands, the conventional model of the so called cylindrical pores [8] relies on a geometry that is not directly related to the physical reality of the polymer framework but that can be used, from the mathematical point of view, for correlating the chromatographic data to the morphology of the polymer framework at the nanometer scale with essentially the same accuracy provided by Ogston's model. As a matter of fact, the porosity of a swollen gel described using cylindrical pore geometry gives easily understandable information about effective size of the cavities among the polymer chains although the pores specific volume data per se might be somewhat erroneous. However, for investigating on the factors affecting the formation of metal nanoclusters inside of the swollen polymer matrix, the effective size of the "cavities" used in the templating molds is much more important than their specific volume.

Results of ISEC characterisation of the swollen state morphology in THF of all MTEMA-DMAA resins are conveniently illustrated in Table 4.

All resins appear to be featured by 0.5 nm domains, the volume of which dominates those relevant to larger cavities (2.5–3.5 nm). Larger "pores" are however well present in MTEMA-DMAA-4–4 and in MTEMA-DMAA-4–6 and albeit scanty, they are observed also in MTEMA-DMAA-4–8. Consequently, on the basis of our TCS model (Fig. 1) [2b], we expect the final production of metal nanoclusters with diameters that correspond to the average size of the largest pores available in the polymer framework in its operational condition. This condition corresponds to the swollen state produced by the liquid medium in which the reduction of the individual metal centers and the consequent formation of size-controlled metal nanoclusters has to occur. Although ISEC analyses for MTEMA-DMAA-10–4 and VAM in water are not available, we reasonably speculate that their nanoporosity is close to that of MTEMA-DMAA-4–4 and poly-methacrylate$^-$ Na^+-divynilbenzene (4% mol) [9].

2.2. XRMA analysis

In the frame of our endeavour to the designed synthesis of topologically well-defined resins/M^0 nanocomposites [2,4,5,10–12], we normally take advantage of X-ray microprobe analysis (XRMA). This simple technique makes it possible to monitor the location of the produced metal nanoclusters ("scanning picture" mode) in the body of the catalyst particles that are normally just submillimetric in size. This convenient technique is featured by ca. 5 μm practical resolution power and provides a useful view of metal distribution normally through equatorial sections of the metallated resins particles (Figs. 3–6).

It is seen that metal nanoclusters dispersion through the body of the support is quite homogeneous in the case of Au^0 and quite inhomogeneous in the case of Pd^0 when the catalyst is prepared from MTEMA-DMAA-4–8 metallated in THF/water. In this last case, metal nanoclusters are seen to

Table 4
ISEC characterisation of macromolecular templates in water

	MTEMA-DMAA-4–4 (ml/g)	MTEMA-DMAA-4–6 (ml/g)	MTEMA-DMAA-4–8 (ml/g)
Sample weight	1.04 g	1.04 g	1.54 g
Dead volume	1.83 ml	1.96 ml	1.22 ml
Pore diameter (nm)			
0.5	1.72	2.16	2.17
1.0	0.00	0.00	0
2.0	0.00	n.d.[a]	0.19
2.5	0.36	0.36	0.79
2.7	0.53	0.39	0.01
3.2	0.51	0.36	0.04
3.5	0.14	0.23	0.06
4.0	0.00	0.01	0.00
Average pore diameter	2.9 nm	2.9 nm	2.5 nm

[a] Not determined.

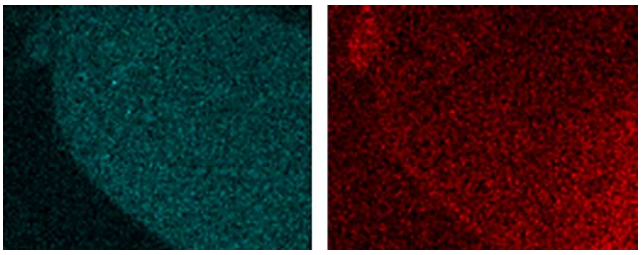

Fig. 3. XRMA scanning picture of MTEMA-DMAA-4–8/Pd: sulfur (left) and palladium distribution (right) (from Ref. [1]) (metallation and reduction in water, see text).

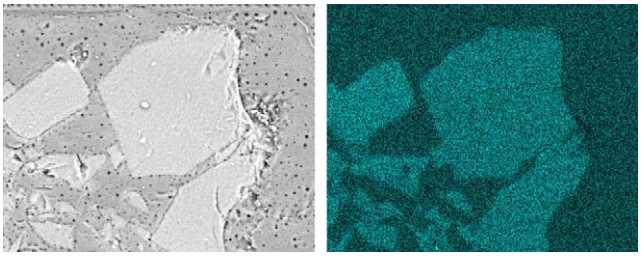

Fig. 4. XRMA scanning picture of MTEMA-DMAA-4–8/Au (right) and SEM picture of the relevant section (left) (from Ref. [1]).

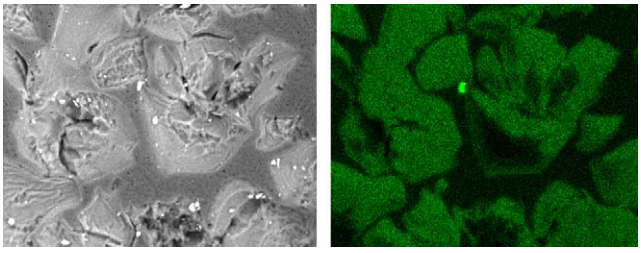

Fig. 5. XRMA scanning picture of MTEMA-DMAA-4–6/Au (right) and SEM picture of the relevant section (left).

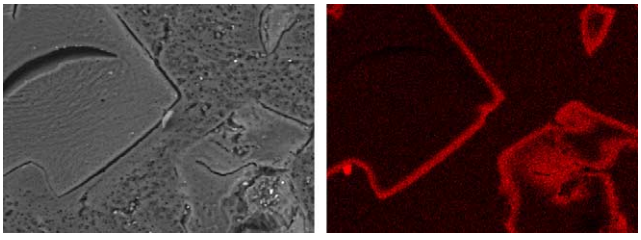

Fig. 6. XRMA scanning picture of MTEMA-DMAA-4–8/Pd (right) and SEM picture of the relevant section (left) (metallation in THF/water and reduction in water, see text).

be located just at the borders of the resin particles in the form of ribbons ca. 20 mm thick (Fig. 6). This seemingly odd observation can be rationalised upon considering that palladiation is carried out with $Pd(OAc)_2$ in a 2:1 THF/water mixture, in which the resin is quite likely swollen by "pure" water (vide infra) [5f]. Consequently, the lipophilic reagent $Pd(OAc)_2$ will be mainly blocked at the periphery of each particle, in spite of the occurrence of a useful concentration gradient towards the interior of the same. Therefore, chemical reduction will take place in the periphery only thus providing a peripheral distribution of palladium nanoclusters. Nothing similar is expected for the case of $AuCl_3$ as it is witnessed by the nice homogeneous metal distribution observed in this case. As to Pd, a far less peripheral distribution is observed for the same support upon using aqueous solutions of $[PdCl_4]^{2-}$ (Fig. 3).

2.3. TEM analysis

As pointed out above, ISEC results lead to the prediction that Au^0 and Pd^0 nanoclusters are present in the reduced resins as really size-controlled spheroidal nanoparticles (Table 5).

The agreement between prediction and observation is seen to be very good for Au^0/MTEMA-DMAA-4–8 and Pd^0/MTEMA-DMAA-4–8 [1] it is good for Pd^0/MTEMA-DMAA-4–4 and poorer for Au^0/MTEMA-DMAA-4–4 (Fig. 7).

2.4. Thermal behaviour of resins MTEMA-DMAA

The thermal behaviour of functional resins is a significant feature for the technological prospects of M^0/resin composites in catalyzed processes. In fact, although in authors opinions the main future applications of these catalysts will be under moderate conditions (typical of fine chemistry and of specialty chemicals syntheses [13]), the important reactions catalyzed by Shi and Deng's catalyst (next paragraph) is carried out at 175 °C [14]. We therefore believe that in systematic synthetic work on polymeric supports, thermal analysis is advisable. Our resins exhibit thermal profiles very little dependent on the cross-linking degree (Fig. 8).

The loss of weight observed up to 100 °C is to be ascribed to the loss of absorbed water. Subsequently the resin is perfectly stable up to 300 °C, at which temperature depolymerization starts to occur. Above this temperature, a second

Table 5
Pd^0 and Au^0 nanoclusters size vs. determined nanoporosity in water (see Table 4)

	MTEMA-DMAA-4–4	MTEMA-DMAA-4–6	MTEMA-DMAA-4–8
Largest available pores (Ref. [2], Fig. 1) (nm)	3.5	3.5	2.5
Metal nanoclusters average diameter (nm)			
Au^0	4.9	n.d.[a]	2.2, 3.3[b]
Pd^0	3.8	n.d.[a]	2.3, 2.6[b]

[a] Not determined.
[b] After 12 months since the preparation of the M^0/Ⓟ catalysts.

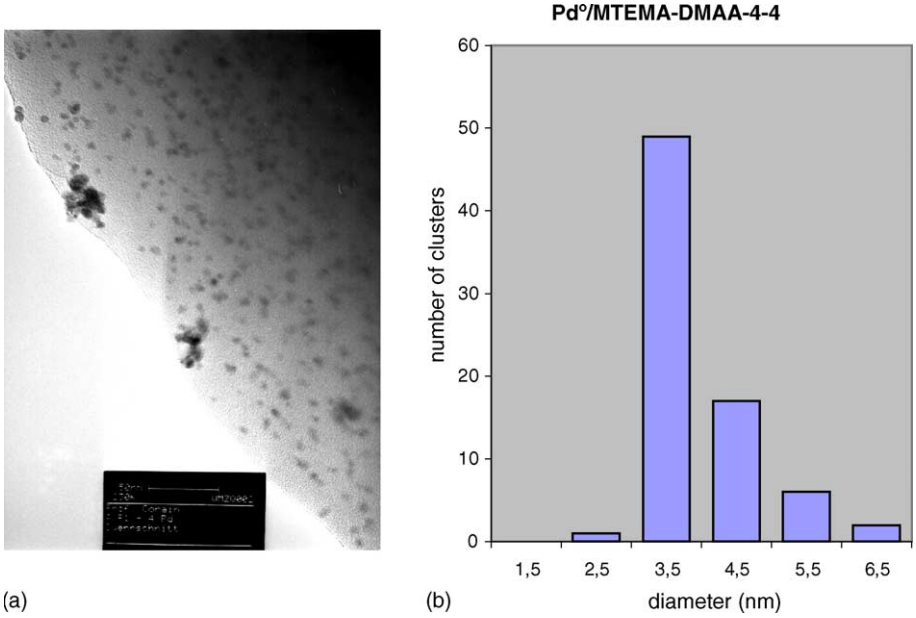

Fig. 7. (a) TEM micrographs of catalyst Pd^0/MTEMA-DMAA-4–4; (b) size distribution of palladium nanoclusters.

seemingly different decomposition step occurs and the complete decomposition of the resin is observed at ca. 700 °C.

2.5. Catalytic tests

Our novel resins-based metal catalysts, when considered at the nanometer scale, differ quite considerably from the traditional ones based on inorganic supports (Fig. 9).

In catalysts (a) the metal nanocluster resides at the external surface of the inorganic framework, while in catalyst (b) the metal nanocluster resides inside of the organic framework where it is "wrapped" (Fig. 2) by an array of polymer chains. In the light of these circumstances, each individual particle of a resin/M^0 composite has to be considered as a sort of microreactor, into which reagents molecules must diffuse from the bulk solution towards the surface of the metal

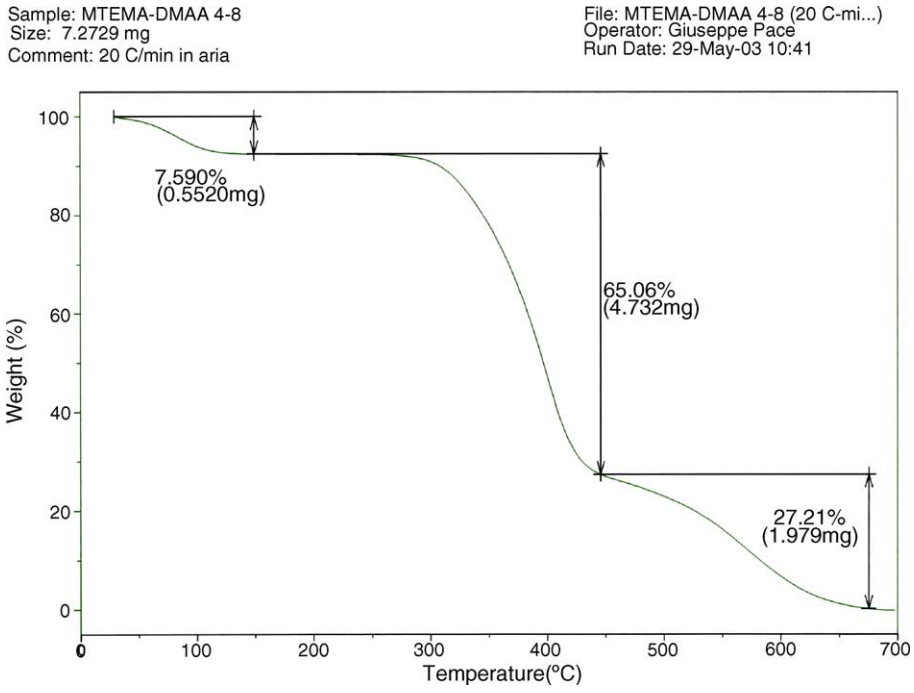

Fig. 8. TGA profile of resin MTEMA-DMAA-4–8 (20 °C/min, under air).

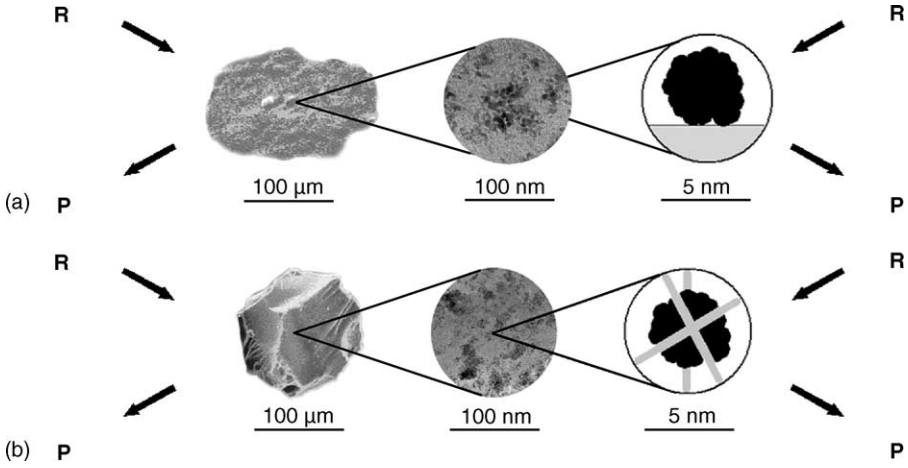

Fig. 9. Metal catalysis on inorganic supports (a) vs. metal catalysis inside an organic polymer framework (b) (see text). R and P denote a reagent molecule migrating from the bulk of the solution to the metal nanocluster surface and a diffusing product molecule, respectively. Distribution of gold through a section of a MTEMA-DMAA-4–6 particle.

nanocluster and from which products molecules must diffuse to reach the bulk of the solution itself.

A very ample documentation stemming from these laboratories reveals that molecular diffusion does not represent in fact a severe kinetic limitation to the reactivity of the interior of the 2–6% cross-linked resin particles, if swollen in a suitable solvent, but simply a circumstance to be considered [5] and rotational and translational mobility of molecules of substantial size turn out to be only moderately affected by microviscosity effects in good swelling solvents [5f].

Catalysts based on nanostructured Au^0 [14] and Pd^0 [15] supported on functional resins have been shown recently to be effective in catalyzing important organic reactions under moderate conditions such as the oxidative carbonylation of amines to carbamates and substituted ureas in the liquid phase [14] and the oxidation of alcohols to aldehydes with molecular oxygen in water, respectively. Shi and Deng did utilize as support a macroreticular commercial resin called Ionexchanger IV (Merck) while Uozumi and Nakao did employ an ad hoc synthesized macroreticular functional resin amphiphilic in nature.

In this work we concentrate our attention on two model oxidation reactions to be carried out with dioxygen in water, i. e. the oxidation of *n*-butanal to *n*-butanoic acid [16] and the selective oxidation of *n*-butanol to *n*-butanal, i. e. a target referring to the class of reactions tested by Uozumi and Nakao [15]. In connection with this second reaction, we have not employed by choice the conditions utilized by the Japanese scientists in ref. [15] (Table 6) and for a suitable evaluation of catalyst potentiality, a metal/substrate ratio equal to 1/1000 mol/mol was employed.

2.6. Oxidation of n-butanal to n-butanoic acid

Under the standard conditions (0.23 M in substrate, substrate/metal = 1000 mol/mol, $p_{O_2} = 3$ atm, 70 °C, reaction time = 2 h) we observe that butanal can be smoothly oxidised to the corresponding acid (Table 6).

Gold supported on MTEMA-DMAA-4–8 appears to be almost twice as active as nanostructured gold on activated carbon. This observation is not surprising on the basis of metal nanoclusters size arguments in heterogeneous catalysis. Moreover, as we have already shown that activity of gold on carbon in liquid phase oxidation reactions could be limited by a shielding effect of carbon itself and small particles may turn out to be less active than larger ones [16b], the ascertained circumstance that in lightly cross-linked resins the framework does not represent a serious limitation to the diffusion of reagents and products [5], strongly suggests that this observation is likely to be a genuine result of a nanoclusters size effect. In general terms, Pd^0 and Au^0 do not exhibit marked difference in reactivity and this is not surprising in view of the fact that palladium(0) has been already shown to be as active as gold(0) when used as the catalyst in aldehyde oxidations [16c,16a].

When bimetallic catalytic systems are employed, we observe a rather surprising effect: Au^0-Pd^0/C proves to be more active than both Au^0/C and Pd^0/C thus proving

Table 6
Oxidation of *n*-butanal[a]

Catalyst	Metal nanoclusters diameter (TEM) (nm)	Conversion (%)
Au^0/MTEMA-DMAA-4–8	2.2	95
Au/C[b]	4.0	42
Pd^0/MTEMA-DMAA-4–8	2.3	89
Pd/C[b]	3.0	44
Au^0-Pd^0/MTEMA-DMAA-10–4	3.5[c]	46
Au^0-Pd^0/C[b]	n.d.[d]	72

[a] Reaction conditions: 0.23 M in substrate, substrate/metal = 1000 mol/mol, $p_{O_2} = 3$ atm, 70 °C, reaction time = 2 h.
[b] From Ref. [16b].
[c] Expected (see text).
[d] Not determined.

Table 7
Oxidation of *n*-butanol[a]

Catalyst	Metal loading (wt%)	Particle diameter (TEM) (nm)	Base	Conversion (%)	Selectivity to aldehyde (%)
Au/MTEMA-DMAA-4–8	0.75	2.2	NaOH	24.6	66.3
			K_2CO_3	33.8	14.4
Au/MTEMA-DMAA-4–4	0.86	4.9	NaOH	13.8	63.3
			K_2CO_3	11.9	42.2
Au/C	1.0	4.0	NaOH	17.4	44.4
			K_2CO_3	28.8	58.2
Au/VAM	0.15	n.d.[b]	NaOH	40	70
Pd/MTEMA-DMAA-4–8	0.70	2.3	NaOH	12.6	60.9
			K_2CO_3	17.5	48.8
Pd/C	1.0	3.0	NaOH	19.6	52.6
			K_2CO_3	24.1	69.7
Au-Pd/MTEMA-DMAA-10–4	2.43 Au	n.d.[b]	NaOH	28.2	55.1
	1.61 Pd		K_2CO_3	41.2	63.2
Au-Pd/C	0.65 Au	2.5	NaOH	94.3	<1
	0.35 Pd		K_2CO_3	84.0	<1

[a] Reaction conditions: 0.23 M substrate, substrate/metal = 1000 mol/mol, substrate/base = 1 mol/mol, pO_2 = 3 atm, 70 °C, reaction time = 2 h.
[b] Not determined.

a synergistic effect between the two metal centers. On the contrary the co-presence of Au and Pd in MTEMA-DMAA-10–4 provokes a detrimental effect with respect to the action of both, individually acting, metal centers.

2.7. Oxidation of n-butanol to n-butanal

The selective oxidation of *n*-alkanols to *n*-aldehydes is a craved goal in organic syntheses [15,17]. This transformation is normally achieved on the basis of a stoichiometric oxidizing approach (vide infra) involving large amounts of toxic oxidizing agents such as compounds of Cr(VI) and Mn(VII). Gold catalysts have been already shown to be active in catalyzing the oxidation of alcohols to acids in the liquid phase [18a] or to aldehydes [18b] in the gas phase. In the liquid phase, the presence of a base is a must for catalytic activity [18a] but it promotes the subsequent oxidation of the intermediate aldehyde to the corresponding carboxylate. High selectivity to aldehyde is expected only in the cases where the aldehyde turns out to be hardly oxidizable *per se*, i.e. for example aromatic ones [16c]. In fact, Uozumi and Nakao observed in the liquid phase [15] that a Pd^0/amphiphilic resin nanocomposite is an active and chemoselective catalyst for the oxidation of non-aliphatic alcohols to aldehydes but they report that their catalyst fails completely in the oxidation of *n*-butanol to butanal that proceeds in fact quantitatively to *n*-butanoic acid.

We report here on the results of the testing of our catalytic materials in the oxidation of *n*-butanol to *n*-butanal in order to determine their activity and selectivity related to the influence of the metal and of the organic support on the chemoselectivity of the process.

Table 7 collects our results of experiments carried out in the presence of different bases (NaOH and K_2CO_3) and a substrate/metal ratio = 1000 mol/mol (T = 70 °C, p_{O_2} = 3 atm). Gold nanoclusters generated inside differently cross-linked resins (in order to form differently sized metal nanoparticles) exhibit the same trend in *activity* as they display in the butanal oxidation reaction, smaller particles being more active than larger ones. The most interesting point, however, deals with the *selectivity* to aldehyde. The presence of a base that normally should enhance overoxidation to carboxylate, does not impede the production of considerable amounts of aldehyde, best results being obtained in the presence of a strong base such as NaOH. Also Pd/C exhibits appreciable reactivity and considerable chemoselectivity to aldehyde.

A quite remarkable result exhibited by one of our catalysts, i.e. Au^0/VAM, is a promising combination of activity (40% conversion) and selectivity to *n*-butanal (70%) [16], VAM being a very hydrophilic resin particularly well suited for operations in water.

The two bimetallic catalysts tested in this work offer another remarkable facet of these catalytic systems. In fact, while Au^0-Pd^0/MTEMA-DMAA-10–4 exhibits an appreciable reactivity and selectivity to *n*-butanal, Au^0-Pd^0/C exhibits a remarkable oxidation activity but a quite disappointing almost 100% selectivity to *n*-butanoate.

3. Conclusions

Catalysts built up with size-controlled Au^0 and Pd^0 nanoclusters located inside the nanoporous domains of copolymers of *N*,*N*-dimethylacrylamide, 2-(methylthio)ethyl methacrylate cross-linked with *N*,*N*′-methylenebisacrylamide appear to be promising candidates for developing dioxygen-based oxidation processes in water solutions. Particularly promising is Au^0 supported on the very hydrophilic resin VAM, as catalyst for the selective oxidation of *n*-butanol to *n*-butanal. Catalysts Au^0/C and Pd^0/C are less active than the M^0/resin counterparts in the oxidation of *n*-butanal to *n*-butanoic acid.

Au^0/C, Pd^0/C, Au^0/resin, Pd^0/resin and Au^0-Pd^0/resin exhibit a moderate activity but a respectable chemoselectivity to *n*-butanal. On the other hand, the bimetallic catalyst Au^0-Pd^0/C turns out to be comparatively very active but leading to the *direct* oxidation of *n*-butanol to *n*-butanoic acid. Apparently, the polymer framework "embracing" the metal nanoclusters in Au^0-Pd^0/MTEMA-DMAA-10–4 (Fig. 9) militates in favour of chemoselectivity to *n*-butanal.

Acknowledgements

This work was partially supported by P.R.I.N. funding 2001–2003, Ministero dell'Università e della Ricerca Scientifica, Italy (project number 2001038991). We are indebted to Dr. K. Jerabek for his supervision to one of us (CB) in Prague and with Company "Programma Ambiente", Padova, Italy for timely and accurate performing of Au and Pd elemental analyses. We are also indebted to Dr. L. Tauro for careful preparation of samples for XRMA and to "Consorzio Interuniversitario nazionale per la Reattività Chimica e la Catalisi" (CIRCC) for a scholarship to one of us (PC).

References

[1] B. Corain, C. Burato, P. Centomo, S. Lora, W. Meyer-Zaika, G. Schmid, J. Mol. Catal. A: Chem. 225 (2004) 189.
[2] (a) F. Artuso, A.A. D'Archivio, S. Lora, K. Jerabek, M. Kralik, B. Corain, Chem. Eur. J. 9 (2003) 5292;
(b) B. Corain, K. Jerabek, P. Centomo, P. Canton, Angew. Chem. In. Ed. 43 (2003) 959.
[3] (a) K. Jerábek, Anal. Chem. 57 (1985) 1595;
(b) K. Jerábek, Anal. Chem. 57 (1985) 1598.
[4] M. Kralik, V. Kratky, M. De Rosso, M. Tonelli, S. Lora, B. Corain, Chem. Eur. J. 9 (2003) 209.
[5] (a) A. Biffis, B. Corain, M. Zecca, C. Corvaja, K. Jerabek, J. Am. Chem. Soc. 117 (1995) 1603;
(b) M. Zecca, A. Biffis, G. Palma, C. Corvaja, S. Lora, K. Jerabek, B. Corain, Macromolecules 29 (1996) 4655;
(c) A.A. D'Archivio, L. Galantini, A. Panatta, E. Tettamanti, B. Corain, J. Phys. Chem. B 102 (1998) 6779;
(d) B. Corain, M. Kralik, J. Mol. Catal. A.: Chem. 159 (2000) 153;
(e) B. Corain, M. Kralik, J. Mol. Catal. A: Chem. 173 (2001) 99;
(f) B. Corain, M. Zecca, K. Jerabek, J. Mol. Catal. A: Chem. 177 (2001) 3;
(g) A. Biffis, R. Ricoveri, S. Campestrini, M. Kralik, K. Jerabek, B. Corain, Chem. Eur. J. 8 (2002) 2962;
(h) B. Corain, P. Centomo, S. Lora, M. Kralik, J. Mol. Catal. A: Chem. 204–205 (2003) 755–762.
[6] M. Kralik, M. Hronec, V. Jorik, S. Lora, G. Palma, M. Zecca, A. Biffis, B. Corain, J. Mol. Catal. A: Chem. 101 (1995) 143.
[7] A.G. Ogston, Trans. Faraday Soc. 54 (1958) 1754.
[8] K. Jerabek, in: M. Potschka, P.L. Dubin (Eds.), Proceedings of the ACS Symposium Series 635, American Chemical Society, Washington, DC, USA, 1996, pp. 211–224.
[9] P. Centomo, S. Lora, M. Zecca, G. Vitulli, A.M. Caporusso, S. Galvagno, C. Milone, B. Corain, J. Catal. 229 (2005) 283.
[10] M. Kralik, V. Kratky, P. Centomo, P. Guerriero, S. Lora, B. Corain, J. Mol. Catal. A: Chem. 195 (2003) 211.
[11] A. Biffis, A.A. D'Archivio, K. Jerabek, G. Schmid, B. Corain, Adv. Mater. 12 (2000) 1909.
[12] B. Corain, P. Guerriero, G. Schiavon, M. Zapparoli, M. Kralik, J. Mol. Catal. A: Chem. 211 (2004) 237.
[13] R.A. Sheldon, H. van, Bekkun (Eds.), Fine Chemicals Through Heterogeneus Catalysis, Wiley, Weinheim, 2001.
[14] F. Shi, Y. Deng, J. Catal. 211 (2002) 548.
[15] Y. Uozumi, R. Nakao, Angew. Chem. Int. 42 (2003) 194.
[16] (a) S. Biella, L. Prati, M. Rossi, J. Catal. (206) (2002) 242, and references therein;
(b) C.L. Bianchi, S. Biella, A. Gervasini, L. Prati, M. Rossi, Catal. Lett. 85 (2003) 91, and references therein;
(b) S. Biella, L. Prati, M. Rossi, J. Mol. Cat. A: Chem. 197 (2003) 207;
(c) S. Coluccia, G. Martra, F. Porta, L. Prati, M. Rossi, Catal. Today 61 (2000) 165.
[17] T. Mallat, A. Baiker, Chem Rev. 104 (2004) 3037.
[18] (a) L. Prati, M. Rossi, J. Catal. 176 (1998) 552;
(b) S. Biella, M. Rossi, Chem. Commun. (2003) 378.